



IMPACT OF ELECTRON RADIATION ON RESISTIVITY IN YBCO AND GdBCO HIGH-TEMPERATURE SUPERCONDUCTING TAPES

Ahmad Abdunabievich Shodiev¹,

Malika Anvarovna Mussaeva¹,

Dilnoza Baxtiyorovna Elmurotova²

¹Institute of Nuclear Physics of the Academy of Sciences of Uzbekistan, M. Ulugbek

District, 100214 Tashkent, Uzbekistan,

E-mail: akhmadshodiyev@gmail.com,

mussaeva@inp.uz. ²Tashkent Medical Academy

E-mail: dilnoza_elmurotova_tma@mail.ru

Abstract

This study investigates the effects of electron radiation on the resistivity and structural properties of second-generation high-temperature superconducting (HTSC) tapes based on $\text{YBa}_2\text{Cu}_3\text{O}_{7-x}$ (YBCO) and $\text{GdBa}_2\text{Cu}_3\text{O}_{7-x}$ (GdBCO). The tapes were subjected to 5 MeV electron irradiation, with doses ranging from 10^{14} to 10^{15} electrons/cm². Structural changes were analyzed using Scanning Electron Microscopy (SEM), Energy Dispersive Spectroscopy (EDS), and X-ray diffraction (XRD), while resistivity measurements were conducted using the Hall effect method. Results indicate that electron irradiation introduces defects such as oxygen vacancies and dislocations, fragmenting crystallites and influencing superconducting properties. GdBCO exhibited higher radiation resistance compared to YBCO, attributed to gadolinium's local magnetic moments, which affect defect formation. The study highlights the potential of radiation-induced defects to enhance vortex pinning and critical current density (J_c) in high magnetic fields, making these materials suitable for applications in fusion reactors, accelerators, and high-field magnets.

Key words: Electron irradiation, HTSC, radiation defects, resistivity, lattice parameter.

Introduction

Modern high-temperature superconducting (HTSC) composite tapes of the second generation, based on $\text{YBa}_2\text{Cu}_3\text{O}_{7-x}$ (YBCO) and $\text{GdBa}_2\text{Cu}_3\text{O}_{7-x}$ (GdBCO) compounds, exhibit high critical current values, making them ideal for applications in electric motors, generators, and current limiters. These materials are also critical components for future fusion power plants, where electromagnetic coils generate intense magnetic fields to confine thermonuclear plasma. However, these coils are subjected to fast





neutron fluxes, which create pinning centers that influence vortex superconductivity [1]. Interestingly, radiation treatment has been shown to restore HTSC tapes by healing crack edges [2].

The effect of radiation on HTSC materials is complex and dose-dependent. For instance, irradiation can lead to non-monotonic changes in the local critical current density (J_c) and the critical temperature of the superconducting transition (T_c). At low doses, J_c may increase, while at high doses, it typically decreases. For example, a study on GdBCO films irradiated with a 6 MeV Zr^{4+} beam demonstrated that optimal fluence and subsequent annealing at 200°C could nearly double J_c in a 5 Tesla magnetic field [3]. Similarly, YBCO and GdBCO tapes irradiated with fast neutrons showed a maximum critical current (I_c) at specific fluences and temperatures (4.2 K) in fields up to 15 Tesla [1].

The radiation resistance of these materials varies depending on the type of irradiating particles. Studies on YBCO and GdBCO tapes irradiated with $^{132}Xe^{27+}$ (167 MeV), $^{84}Kr^{17+}$ (107 MeV), $^{40}Ar^{8+}$ (48 MeV) ions, and 2.5 MeV protons revealed that GdBCO exhibits higher radiation resistance compared to YBCO [4]. Calculations using the SRIM and thermal peak models estimated the sizes of radiation-induced defects, which serve as pinning centers for Abrikosov vortices. For example, argon ions create defects of approximately 5 nm, while krypton and xenon ions produce defects of 6.2 nm and 6.8 nm, respectively [4].

GdBCO has shown superior performance in high magnetic fields. Long (>50 m) coated conductors and coils based on GdBCO demonstrated higher J_c values compared to YBCO. A 4-turn, 83-layer solenoid coil with a GdBCO conductor achieved a central magnetic field of 5.68 T at 4.2 K, highlighting its potential for high-field applications [5]. Further improvements were achieved by adding 15% Zr to (Gd, Y)-Ba-Cu-O tapes, enhancing pinning in magnetic fields up to 30 Tesla [6]. Additionally, non-stoichiometric GdBCO films with a 15% excess of Gd exhibited thread-like defects of the non-superconducting phase Gd_2CuO_4 , which altered the vortex pinning mechanism and resulted in a distinct critical current peak [7].

Previous studies on YBCO microfilms irradiated with a 5 MeV electron beam revealed significant structural modifications at the YBCO-AgCu interfaces. This irradiation led to a tenfold reduction in magnetoresistance above T_c , an increase in the steepness of the superconducting transition, and a dramatic decrease in charge carrier mobility (μ) at temperatures below 100 K and above 280 K, where Cooper pairs and magnons condense, respectively [8,9].

The crystal structures of YBCO and GdBCO are similar, with Gd introducing a local magnetic moment due to its intrinsic spin (3.62–10.5 μ_B), unlike non-magnetic



yttrium. Despite this, the critical temperatures (T_c) of these compounds differ by no more than 3 K [10]. Table 1 summarizes the unit cell dimensions of the most common superconducting cuprates [11].

Table 1. Unit cell dimensions of common superconducting cuprates [10, 11]

Compound	a (Å)	b (Å)	c (Å)
YBCO	3.8227	3.8872	11.6802
GdBCO	3.837	3.677	11.786
NdBCO	3.911	3.913	11.725

Replacing YBCO with GdBCO in solenoid cables has enabled the maintenance of superconductivity in magnetic fields exceeding 10 T at 4.2 K, opening new possibilities for accelerator technology [6].

The aim of this study is to investigate the effects of electron radiation on the resistivity and structural properties of second-generation high-temperature superconducting (HTSC) tapes based on $\text{YBa}_2\text{Cu}_3\text{O}_{7-x}$ (YBCO) and $\text{GdBa}_2\text{Cu}_3\text{O}_{7-x}$ (GdBCO).

Research Methods

Objects of Study: The study focuses on 2nd generation high-temperature superconducting (HTSC) tapes. These tapes consist of a 5–8 μm thick layer of superconducting material, either YBCO (Yttrium Barium Copper Oxide) or GdBCO (Gadolinium Barium Copper Oxide), deposited on a ferromagnetic steel substrate (S-276, Ni-Cr-Fe alloy). The steel substrate has a thickness of 60 μm and a width of 4 mm. The tapes are further enhanced with a nanostructured insulating multilayer coating and are coated with metallic layers: 3 μm of silver (Ag), 4 μm of copper (Cu), and 4 μm of lead-tin alloy (PbSn) [12].

These tapes, manufactured by SuperOx (a collaboration between S-Innovations, Russia, and Japan; www.superox.ru) [13], are designed to carry currents exceeding 200 A at 4.2 K in a 10 Tesla magnetic field. Two specific variants of these tapes are SuperOx-1 YBCO and SuperOx-3 GdBCO, which are optimized for high-performance applications in extreme conditions.

Electron irradiation: Tape samples, cut into 5 cm long segments, were mounted parallel to the direction of the electron beam scanning. The irradiation was conducted at 273 K (in the non-superconducting state) using the “Electronics U-003” accelerator at the Institute of Nuclear Physics, Academy of Sciences of the Republic of Uzbekistan.



The samples were exposed to an electron beam with an energy of 5 MeV, ensuring that the electrons penetrated through the 10 μm thick coating layers and reached the superconducting layer [14].

The irradiation was performed at three different fluences:

$1 \cdot 10^{14}$ electrons/ cm^2 and $5 \cdot 10^{14}$ electrons/ cm^2 at a current density of 400 nA/ cm^2 ,
 $1 \cdot 10^{15}$ electrons/ cm^2 at a current density of 1 mA/ cm^2 ,

These conditions were selected to study the effects of electron irradiation on the superconducting properties and structural integrity of the tapes.

Methodology:

The microstructure and local elemental composition of the internal high-temperature superconducting (HTSC) microlayer were analyzed using the Scanning Electron Microscopy (SEM) - Energy Dispersive Spectroscopy (EDS) method on an EVO-MA 10 electron microscope (Zeiss). To achieve this, a cross-section of the tape was prepared, and areas where the metal coatings had peeled off from the HTSC layer were identified (Fig. 1-2).

Non-destructive X-ray diffraction (XRD) analysis of the tapes was performed on the side of the HTSC layer with the three-layer metal coating using an Empyrean diffractometer (PANalytical, Netherlands). The phase composition was determined using the PDF-2016 database.

The resistivity (ρ , $\Omega \cdot \text{cm}$) was measured using a gold-coated, four-point probe method in conjunction with Hall Effect measurements, employing the HMS-7000 system and the AMP55T magnet kit (Ecopia, South Korea) for low-temperature measurements (80K–350K). The theoretical basis of the Hall Effect measurement is the Lorentz force and the Van der Pauw technique, which provides precise resistivity and charge carrier mobility data. Measurements were conducted under a magnetic field of $B = 0.556$ T and a current of $I = 10$ mA.

Results and Discussion:

Microstructure Analysis (Fig. 1, left image). The SEM image reveals the interfaces between different layers, including YBCO, Ag, Cu, and buffer layers. These interfaces exhibit irregularities at the microscale, which may serve as chemical pinning centers in the SuperOx-1 tape. Grain boundaries and structural defects within these layers can influence superconducting properties, particularly critical current density (J_c) and vortex dynamics.



The layered architecture plays a fundamental role in the flux pinning mechanism, which is essential for maintaining stable superconducting currents in external magnetic fields. The irregularities at the interfaces could enhance vortex pinning, thereby improving performance in high-field applications such as superconducting magnets, fusion reactors, and particle accelerators.

Microlocal Elemental Composition (Fig. 1, right image). Spectrum 114 confirms the presence of $\text{YBa}_2\text{Cu}_3\text{O}_7$ (YBCO), the superconducting phase, with stoichiometric oxygen concentration, which directly determines its critical temperature (T_c). The elemental composition analysis identifies additional elements present in the coatings and substrate, including Pb, Sn, Ag, Cu, and Ni-Cr-Fe, which contribute to mechanical strength and electrical properties. Oxygen vacancies in YBCO can lead to charge carrier depletion, which negatively impacts T_c and resistivity. The presence of Ag and Cu coatings enhances mechanical stability and improves electrical contact, but it may also influence electron scattering and surface resistivity. Since Figure 1 represents the initial, unirradiated state of YBCO, it provides a baseline for comparison with irradiated samples to analyze how electron radiation alters the microstructure and composition.

Spectra 273–280 were measured at designated positions, covering the YBCO layer and its interfaces with the coatings and buffer nanolayers on the steel substrate. Spectrum 274 shows fragments of Pb melt on a continuous Sn film, indicating PbSn alloy decomposition due to intensive irradiation. Spectra 273 and 275 correspond to the bilayered Cu and Ag coatings on the superconducting YBCO layer.

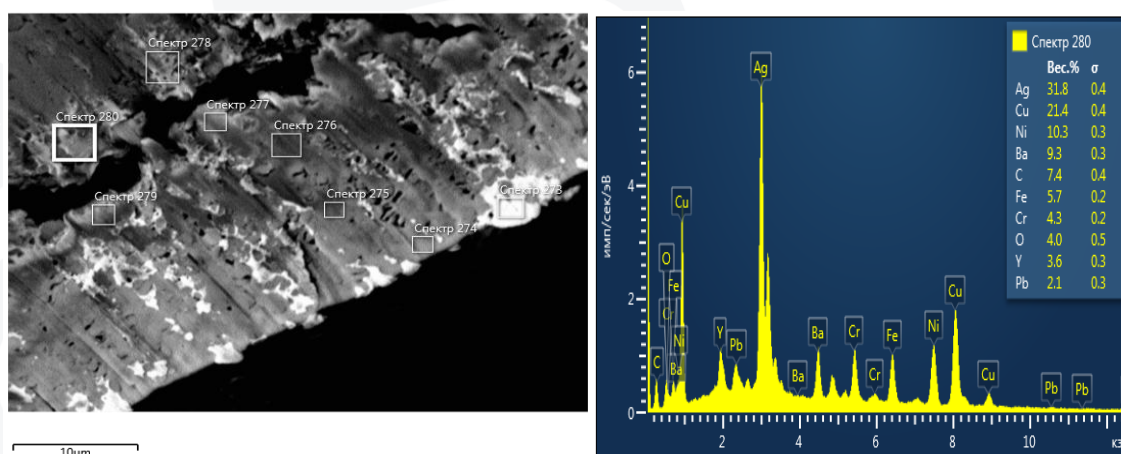


Fig.1. Microstructure (left) and microlocal elemental composition (right) of mixed layers on the lateral cross-section YBCO tape.

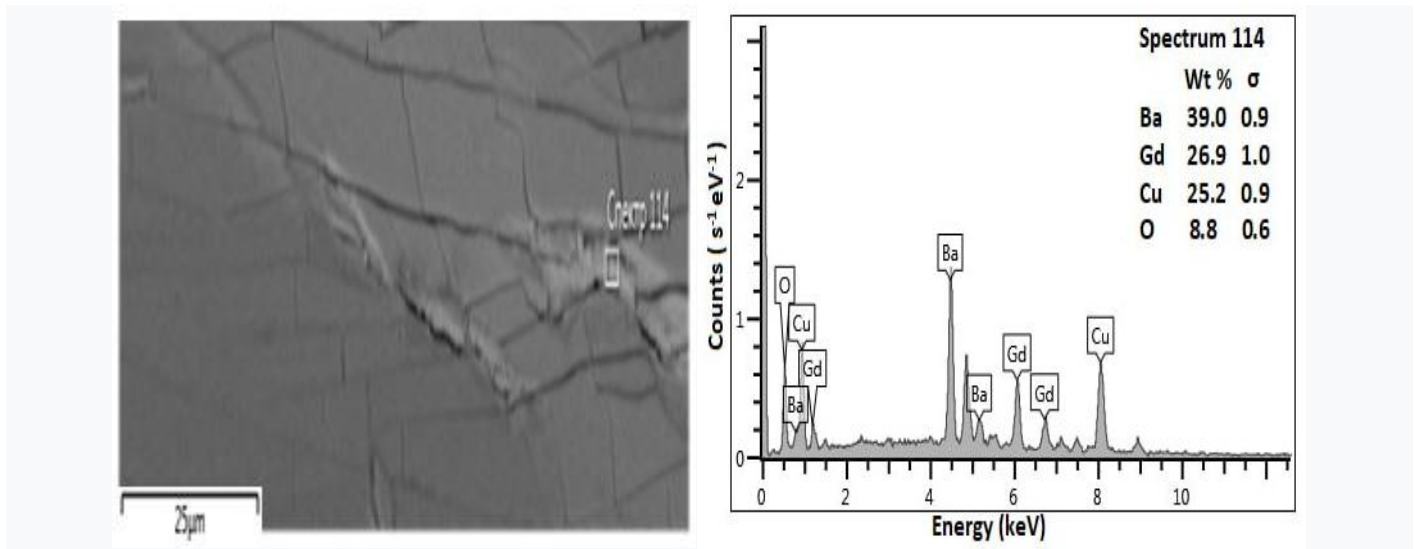


Fig.2. SEM image of a superconducting crystalline layer (left), showing the localization of the electron beam for recording the characteristic spectrum, and (right) the measured local EMF spectrum.

SEM-EDS Analysis: Microstructure and Local Elemental Composition of GdBCO (Fig. 2) Figure 2 presents the SEM microstructure and EDS local elemental composition of GdBCO tapes: The left image depicts a superconducting monocrystalline layer, highlighting the electron beam localization for recording the characteristic X-ray spectrum (shown in the right image). Spectrum 114 confirms the stoichiometric elemental composition of $\text{GdBa}_2\text{Cu}_3\text{O}_7$ (GdBCO). The superconducting phase has a measured critical temperature (T_c) of 91 K, corresponding to an oxygen vacancy concentration of <0.1 at./mol. The layered structure of GdBCO promotes the growth of lamellar single crystallites, which are up to $20 \mu\text{m}$ in length and $5 \mu\text{m}$ in thickness. These crystallites exhibit linear shapes at their coherent boundaries, influencing the vortex pinning mechanism and overall superconducting performance.

XRD Analysis of the Multilayer Tape X-ray diffraction (XRD) analysis was performed from the side of the HTSC layer, based on the penetration depth of the X-ray radiation (Cu cathode, up to $20 \mu\text{m}$). Dielectric nanolayers and the steel substrate were not detected.

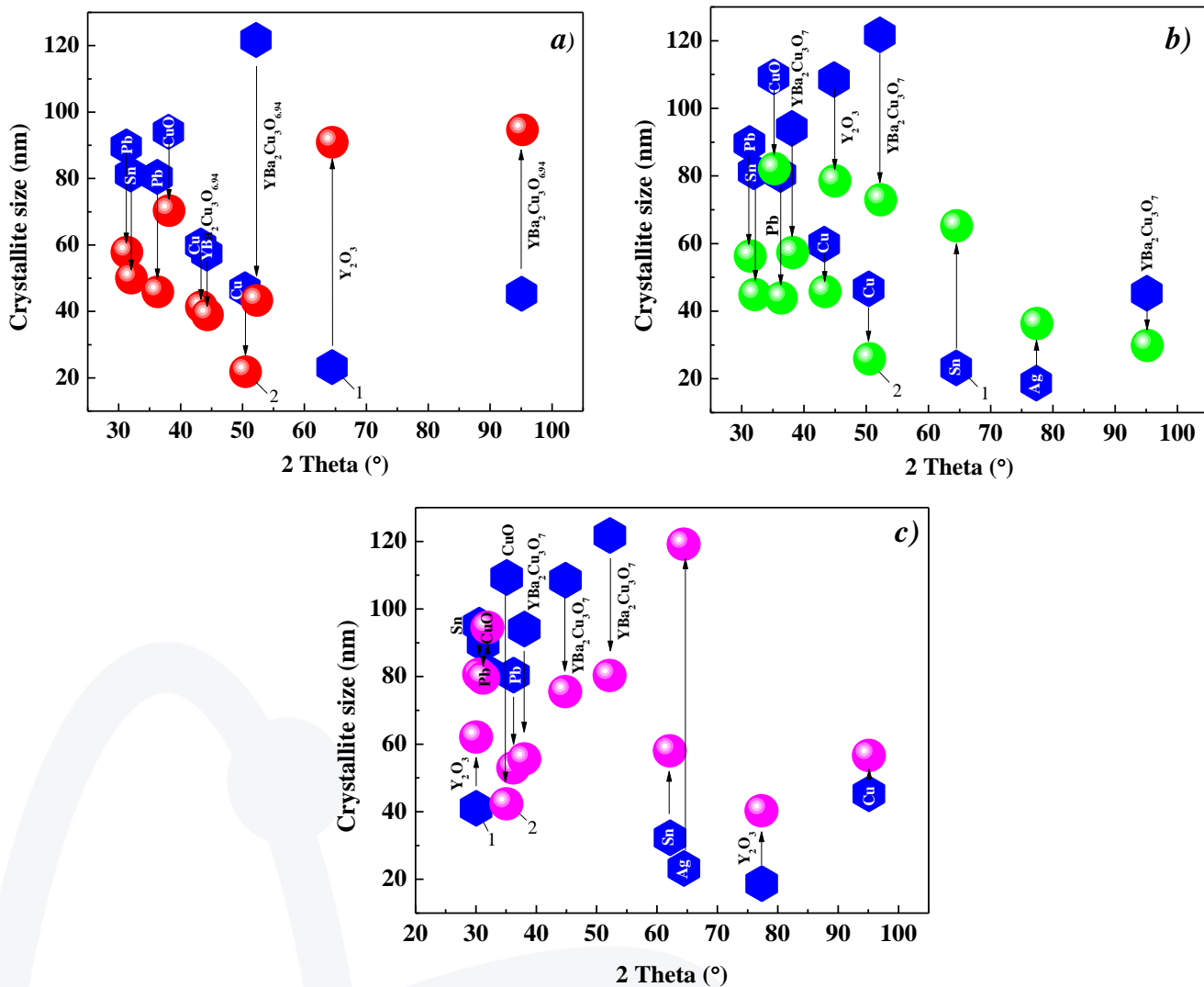


Fig.3. Crystallite size calculated by XRD spectra of SuperOx-1 YBCO tape: 1 – reference, 2– immediately after irradiation with 5 MeV electrons at a current density of 400 nA/cm² at doses of (a) – 10¹⁴ cm⁻², (b) – 5·10¹⁴ cm⁻² and (c) – 10¹⁵ cm⁻² at a current density of 1 μA/cm²

The Fig.3. compares the crystallite size of YBCO tapes before (reference) and after irradiation with 5 MeV electrons at different doses: 10¹⁴ cm⁻², 5 · 10¹⁴ cm⁻², and 10¹⁵ cm⁻². The crystallite size is calculated from XRD spectra, which provide information about the structural changes in the material. Crystallite size is a measure of the average size of coherently diffracting domains in the material. Smaller crystallites indicate more grain boundaries and defects. Electron irradiation introduces defects (e.g., oxygen vacancies, dislocations) that can fragment larger crystallites into smaller ones, reducing the overall crystallite size. At lower doses (e.g., 10¹⁴ cm⁻²), the crystallite size may decrease slightly due to the introduction of point



defects (e.g., oxygen vacancies). At higher doses (e.g., 10^{15} cm^{-2}), the crystallite size may decrease significantly due to the formation of extended defects (e.g., dislocations, voids) and recrystallization at grain boundaries. Smaller crystallites and increased defects can act as pinning centers for Abrikosov vortices, enhancing the critical current density (J_c) in certain magnetic fields. However, excessive defects can also disrupt the superconducting phase, leading to a decrease in J_c and T_c (critical temperature).

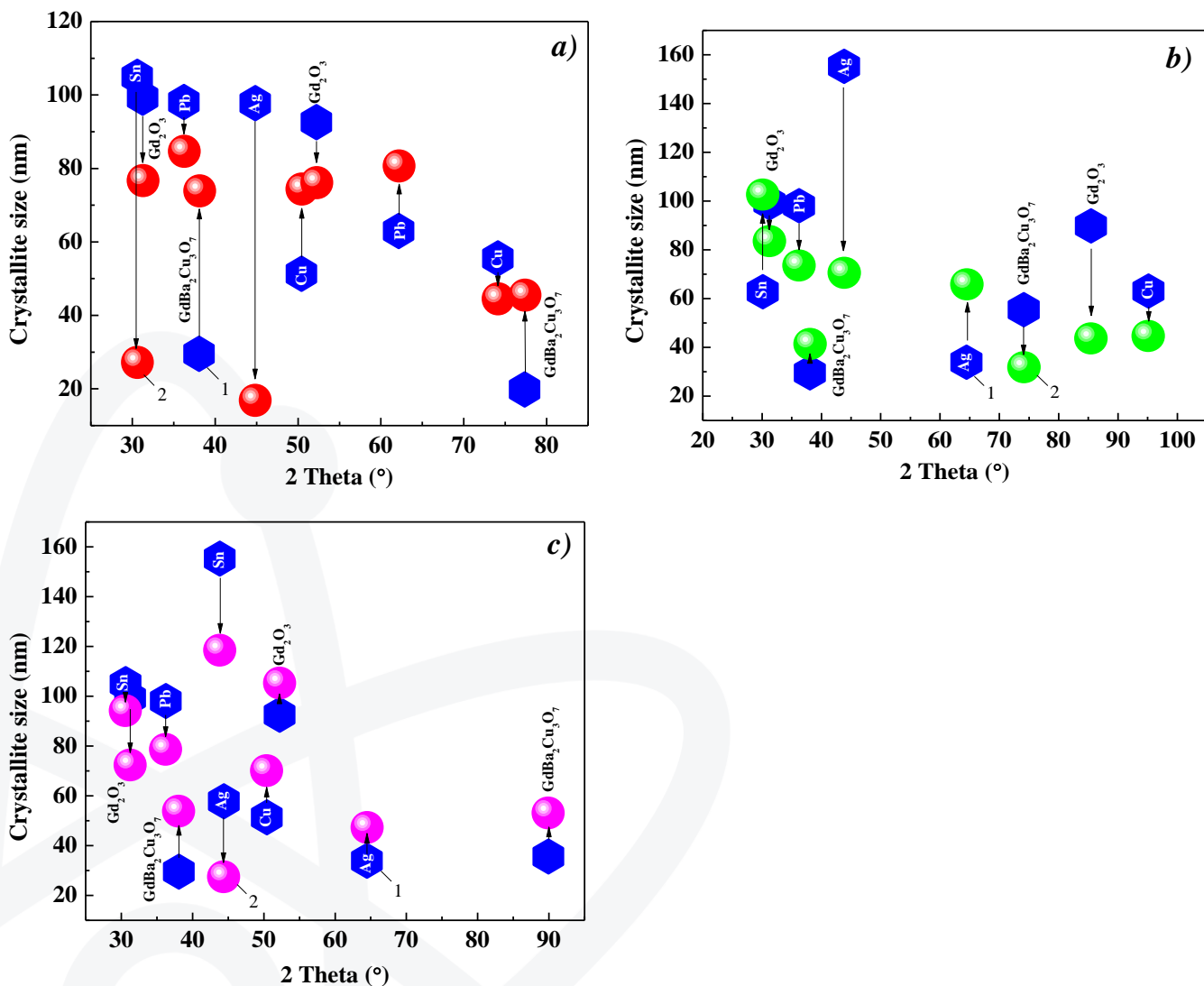


Fig.4. Crystallite size calculated by XRD spectra of SuperOx-3 GdBCO tape: 1 – reference, 2– immediately after irradiation with 5 MeV electrons at a current density of 400 nA/cm² at doses of (a) – 10^{14} cm^{-2} , (b) – $5 \cdot 10^{14} \text{ cm}^{-2}$ and (c) – 10^{15} cm^{-2} at a current density of $1 \mu\text{A/cm}^2$



Fig.4. Crystallite size in SuperOx-3 GdBCO tape similar to Fig.3., this figure shows the crystallite size of GdBCO tapes before (reference) and after irradiation with 5 MeV electrons at the same doses: 10^{14} cm^{-2} , $5 \cdot 10^{14} \text{ cm}^{-2}$, and 10^{15} cm^{-2} . GdBCO tapes contain gadolinium (Gd), which introduces local magnetic moments due to its intrinsic spin. This can influence the pinning of vortices and the overall superconducting properties. Gd also affects the formation of defects under irradiation, as it can interact differently with radiation compared to yttrium (Y) in YBCO.

Electron irradiation in GdBCO creates defects such as oxygen vacancies and interstitial oxygen ions. These defects can order into a sublattice, which may enhance vortex pinning and improve J_c . The crystallite size in GdBCO may show a different trend compared to YBCO due to the presence of Gd and its interaction with radiation. At lower doses, the crystallite size may decrease slightly, similar to YBCO, but the presence of Gd could lead to unique defect configurations. At higher doses, the crystallite size may decrease more significantly, but the formation of Gd_2O_3 nanophases (as mentioned in the article) could provide additional pinning centers, improving J_c in high magnetic fields.

GdBCO generally exhibits higher radiation resistance compared to YBCO, as mentioned in the article. This is reflected in the crystallite size trends, where GdBCO may maintain better structural integrity under irradiation. The decrease in crystallite size after irradiation indicates the introduction of defects, which can act as pinning centers for vortices, enhancing J_c in certain conditions. Low doses of irradiation introduce point defects (e.g., oxygen vacancies), while high doses cause extended defects and recrystallization, both of which influence the superconducting properties. YBCO and GdBCO respond differently to irradiation due to the presence of Gd in GdBCO, which introduces magnetic moments and influences defect formation.

Understanding the crystallite size and defect structure helps optimize the performance of HTSC tapes for applications like fusion reactors, accelerators, and high-field magnets.

XRD analysis identifies the crystalline structure and estimates its volume in % only for crystalline phases, while amorphous phases are visible as a weak broad scattering band at small angles and are not included in the phase calculation. Non-irradiated samples contain interface nanophases Gd_2O_3 , providing a high current in a magnetic field. This confirms that the centers of chemical pinning in non-irradiated ribbons are oxide nanophases at the interfaces of HTSC tapes [1,3,7]. After electron irradiation to 10^{15} cm^{-2} , the ratio of Gd_2O_3 to $\text{GdBa}_2\text{Cu}_3\text{O}_7$ increased from 2 to 2.5 times, and irradiation also caused recrystallization of the coating interfaces.



The fig.5. compares the resistivity (ρ) of YBCO and GdBCO tapes as a function of temperature before (reference) and after irradiation with 5 MeV electrons at different doses: 10^{14} cm^{-2} , $5 \cdot 10^{14} \text{ cm}^{-2}$, and 10^{15} cm^{-2} .

YBCO tape, reference curve resistivity increases from $\mu\Omega\cdot\text{cm}$ to $\text{m}\Omega\cdot\text{cm}$ as the temperature rises to 180 K, marking the onset of the superconducting transition. At 240 K, resistivity drops sharply to $10 \mu\Omega\cdot\text{cm}$, indicating another transition, before increasing again at higher temperatures. The initial increase in resistivity is due to the thermal activation of charge carriers as the material transitions from the superconducting to the normal state. The sharp drop at 240 K suggests a secondary transition, possibly related to changes in the oxygen vacancy ordering or structural phase transitions in the CuO chains.

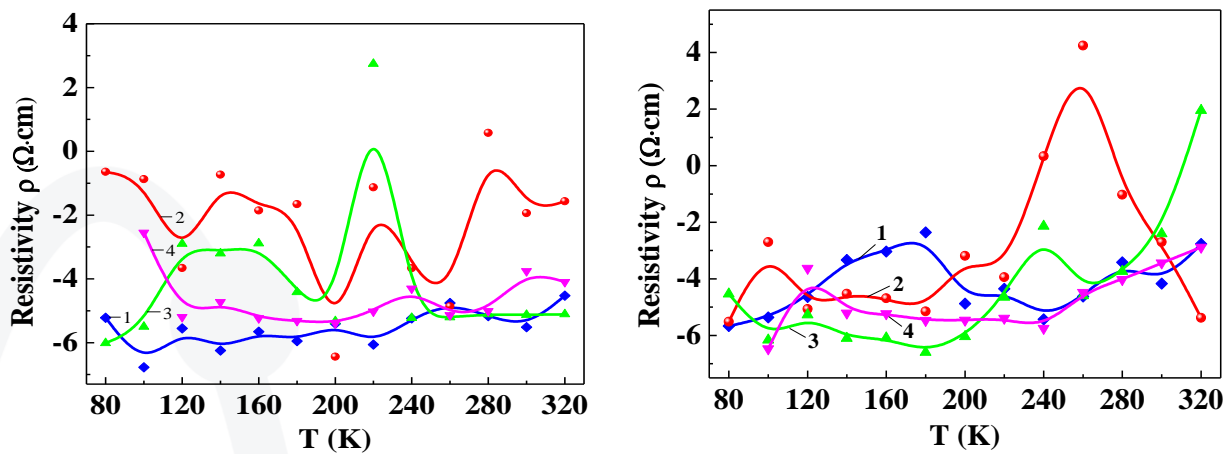


Fig.5. Temperature dependence of resistivity (ρ) for YBCO (left) and GdBCO (right) tapes. 1 – reference, irradiated with 5 MeV electrons at 273 K to a doses of ($2 - 10^{14} \text{ cm}^{-2}$ [8], 3 – $5 \cdot 10^{14} \text{ cm}^{-2}$, 4 – 10^{15} cm^{-2}).

In Fig.5 irradiated curves, low dose (10^{14} cm^{-2}) resistivity peaks at 100 K (onset of superconductivity) and 260 K, indicating significant changes in the material's electronic structure. The increase in resistivity at these temperatures suggests the introduction of defects (e.g., oxygen vacancies) that disrupt the superconducting phase. Medium dose ($5 \cdot 10^{14} \text{ cm}^{-2}$), the resistivity trend is similar but less pronounced, indicating a saturation of defect formation. High dose (10^{15} cm^{-2}), the onset of superconductivity shifts to 120 K, and resistivity decreases in the range of 140–240 K. This suggests that high-dose irradiation induces ordering of oxygen vacancies and interstitial oxygen ions, enhancing conductivity in certain temperature ranges. GdBCO tape reference curve similar to YBCO, resistivity increases with temperature, but the transitions may occur at slightly different temperatures due to



the presence of gadolinium (Gd). Gd introduces local magnetic moments, which can influence the pinning of vortices and the overall superconducting properties. The resistivity trends reflect the interplay between superconductivity and magnetic interactions in GdBCO. Irradiated curves, low dose (10^{14} cm^{-2}), resistivity peaks at 100 K and 260 K, similar to YBCO, but the presence of Gd may lead to a more pronounced decrease in resistivity due to enhanced defect ordering. Medium dose ($5 \cdot 10^{14} \text{ cm}^{-2}$), the resistivity trend is similar but less pronounced, indicating a saturation of defect formation. High dose (10^{15} cm^{-2}), resistivity decreases significantly in the range of 100–200 K, indicating improved conductivity. This is attributed to the formation of ordered oxygen vacancies and interstitial oxygen ions, which enhance charge carrier mobility. Electron irradiation creates oxygen vacancies and interstitial oxygen ions in the CuO chains. These defects can order into a sublattice, reducing resistivity by improving charge carrier mobility and providing additional pathways for current flow. Low doses introduce point defects (e.g., oxygen vacancies), while high doses cause extended defects and recrystallization, both of which influence resistivity and superconducting transitions. YBCO and GdBCO respond differently to irradiation due to the presence of Gd in GdBCO, which introduces magnetic moments and influences defect formation. Understanding the resistivity trends helps optimize the performance of HTSC tapes for applications like fusion reactors, accelerators, and high-field magnets. For YBCO resistivity peaks at 100 K and 260 K, with a decrease at higher doses. For GdBCO similar peaks but with a more pronounced decrease in resistivity at higher doses.

Conclusions

The study demonstrates that electron irradiation significantly impacts the structural and electrical properties of YBCO and GdBCO HTSC tapes. Electron irradiation introduces defects such as oxygen vacancies and dislocations, leading to a reduction in crystallite size and changes in resistivity. GdBCO tapes exhibited higher radiation resistance compared to YBCO, likely due to the presence of gadolinium, which influences defect formation and vortex pinning. The formation of ordered oxygen vacancies and interstitial oxygen ions at higher irradiation doses improved conductivity in certain temperature ranges, particularly in GdBCO. These findings suggest that controlled electron irradiation can optimize the performance of HTSC tapes for applications in extreme radiation environments, such as fusion reactors and high-field magnets. The study provides valuable insights into the role of gadolinium in defect formation and the potential for enhancing the superconducting properties of HTSC materials through electron radiation treatment.





References

1. Fischer D. X, Prokopec R, Emhofer J, Eisterer M. The effect of fast neutron irradiation on the superconducting properties of REBCO coated conductors with and without artificial pinning centers // *Supercond. Sci. Technol.* 2018. 31. 044006 (8 pp). doi.10.1088/1361-6668/aaadf2.
2. Podlivaev A.I., Rudnev I.A. Radiation treatment of the crack edges of the superconducting layer during the restoration of HTSC tape // *Solid State Physics*, 2022, Volume 64, No.3. pp.319–325. doi:10.21883/FTT.2022.03.52092.233.
3. Haberkorn N., Suárez S., Lee Jae-Hun, Moon S.H., Lee Hunju. In-field dependences of the critical current density J_c in $GdBa_2Cu_3O_{7-d}$ coated conductors produced by Zr irradiation and post-annealing at low temperatures // *Solid state communications* 2019, Vol. 289, P. 51–55. doi.org/10.1016/j.ssc. 2018.12.008.
4. Troitsky A.V., Demikhov T.E., Antonova L.Kh., Didyk A. Yu, Mikhailova G.N. Radiation effects in composite high-temperature superconductors. // *Surface. X-ray, synchrotron and neutron studies.* 2016. No. 4. pp.18–30. doi:10.7868/S020735281604020X.
5. Fukushima H, Ibi A, Takahashi H, Kuriki R, Miyata S, Yamada Y, Shiohara Y. GdBCO and YBCO long coated conductors and coils. // *Physica C.* 2007. Vol. 463–465. P. 501–504. https://doi.org/10.1016/j.physc.2007.04.238.
6. Xu A., Delgado L., Khatri N., Liu Y., Selvamanickam V., Abraimov D., Jaroszynski J., Kametani F., and Larbalestier D.C. (2014). Strongly enhanced vortex pinning from 4 to 77 K in magnetic fields up to 31 Tesla in 15 mol.% Zr-added (Gd,Y)-Ba-Cu-O superconducting tapes. *Applied Phys. Lett. Mater.* 2(4): 046111. https://doi.org/10.1063/1.4872060.
7. Degtyarenko P.N., Sadakov A.V., Ovcharov A.V., Degtyarenko A.Yu., Gavrilkin S.Yu., Sobolevsky O.A., Tsvetkov A.Yu., Massalimov B.I. Effect of Gd concentration on superconducting properties in 2nd generation HTSC tapes // *JETP Letters*, 2023, Vol. 118. Issue 8. pp.590–595. doi: 10.31857/S1234 567823200077.
8. Ibragimova E. M., Mussaeva M. A., Shodiev A. A., Iskandarov N. E. and Nazarov K. T. Microstructure, magnetoresistivity and carrier mobility of HTSC-YBCO tape with pinning centers generated by electron irradiation // *Journal of Physics: Conference Series. AAPM -2023.* 2573. (2023). R.1–7. 012013 doi:10.1088/1742-6596/2573/1/012013.
9. E.M. Ibragimova, A.A. Shodiev, S. Ahrorova, M.A. Mussaeva, N.E. Iskandarov, U.T. Kurbanov, M.Yu. Tashmetov. Low-dimensional magnetic centers in HTSC-



- YBCO film on steel-276 induced by gamma-quanta and electron beam. Journal of Magnetism and Magnetic Materials 595 (2024) 171617.
10. Physical properties of high-temperature superconductors: [Collection of articles] / Ed. D. M. Ginsberg; Per. from English edited by N.V. Zavaritsky. – Moscow: Mir, 1990. 543 p
 11. Bondarenko S.I., Koverya V.P., Krevsun A.V., Link S.I. High-temperature superconductors of the (RE)Ba₂Cu₃O₇₋₈ family and their applications // Low Temperature Physics / Physics of low temperatures. 2017. Vol.43. No.10. S.1411–1445.
 12. A.A. Shodiev, M.A. Mussaeva, N.R. Nishonova, D.B. Elmurotova, D.X. Islamova. Improving structure and superconductivity of coated cuprate tapes by irradiation with electrons and gamma-rays. Nanotechnology Perceptions ISSN: 1660-6795, Vol. 20 No.7 (2024) pp. 209-216.
 13. Mikhailova G.N., Voronov V.V., Troitsky A.V., Didyk A.Yu., Demikhov T.E., Suvorova E.I. Processing method for high temperature superconductor. Patent RF. 2013. No.2477900.
 14. A.A. Shodiev, M.A. Mussaeva, D.B. Elmurotova. Magnetic resistance and mobility of carriers of HTSC - YBCO tapes irradiated with 5 MeV electrons. Eurasian Journal of Physics, Chemistry and Mathematics. ISSN: 2795-7667, Volume 35, October 2024, IF:7.825, 25-33 p.p.

